Electronic Supplementary Information (ESI)

Large Stress Asymmetries of Lipid Bilayers and Nanovesicles Generate Lipid Flip-Flops and Bilayer Instabilities

Aparna Sreekumari and Reinhard Lipowsky*

Theory and Biosystems, Max Planck Institute of Colloids and Interfaces, Science Park Golm, 14424 Potsdam, Germany

May 15, 2022

This Supporting Information contains seven figures, seven tables, and three movie captions.

Figures:

– Figs. S1, S2, and S4 with stress profiles across planar bilayers and nanovesicles;
– Figs. S3 and S5 with Weibull plots for the large and small nanovesicles;
– Fig. S6 illustrating the instability of a small nanovesicle; and
– Fig. S7 with the master curve for the onset of flip-flops within nanovesicles.

Tables:

– Tables S1 and S2 with numerical parameter values for planar bilayers;
– Tables S3 and S4 with numerical parameter values for larger nanovesicles;
– Tables S5 and S6 with numerical parameter values for smaller nanovesicles; and
– Table S7 with the stability regimes in terms of the torque densities.

Movie captions:

– Time-lapse Movie 1 with structural instability and self-healing process of a planar bilayer;
– Time-lapse Movie 2 with structural instability and self-healing process of a large nanovesicle; and
– Time-lapse Movie 3 with structural instability and self-healing process of a small nanovesicle.

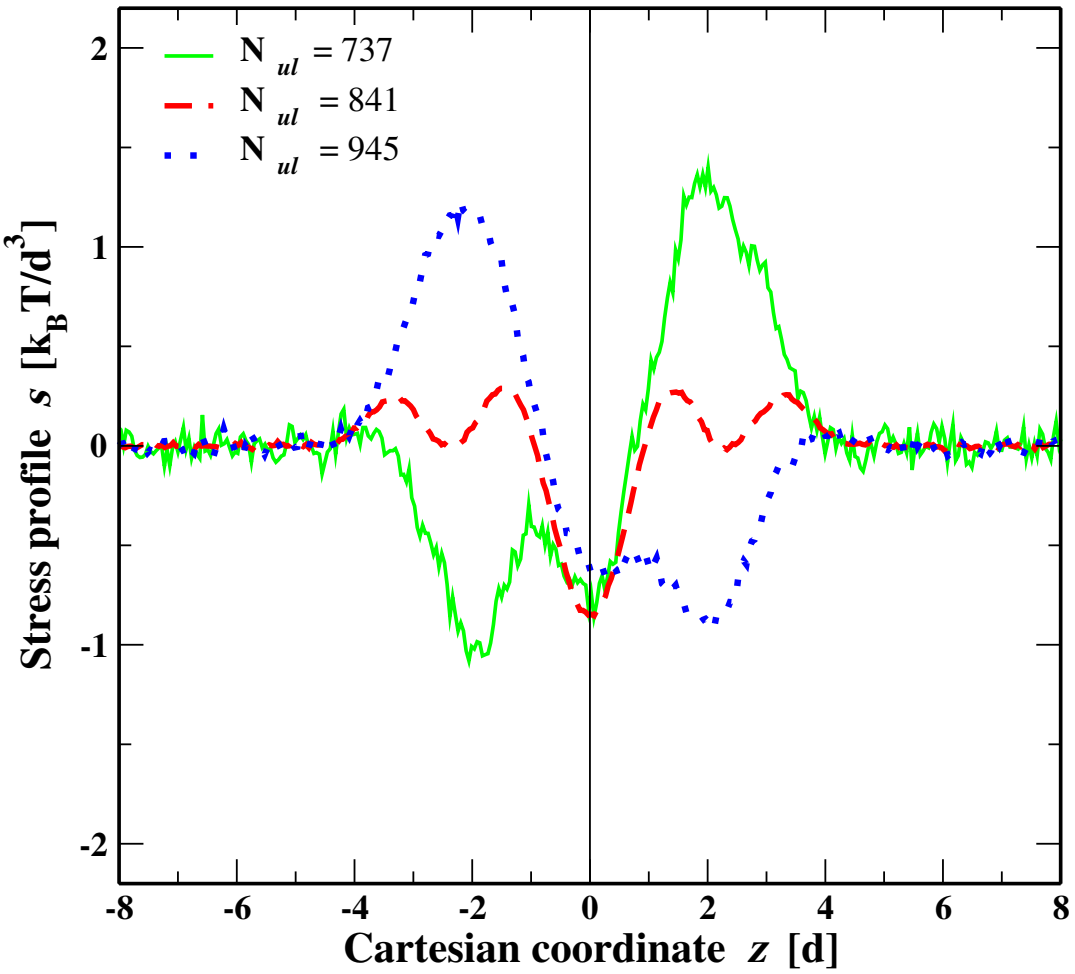

Figure S1: Stress profiles s across three planar and tensionless bilayers versus the Cartesian coordinate z perpendicular to these bilayers. Each bilayer is assembled from N_{ul} lipids in the upper leaflet with $z > 0$ and $N_{ll} = 1682 - N_{ul}$ lipids in the lower leaflet with $z < 0$. The three profiles are obtained for $N_{ul} = 737$ (solid green line), corresponding to a stretched upper leaflet and a compressed lower one; $N_{ul} = 841$ (dashed red line), corresponding to two tensionless leaflets; and $N_{ul} = 945$ (dotted blue line) corresponding to a compressed upper leaflet and a stretched lower one. The numerical values of the corresponding leaflet tensions Σ_{ul} and Σ_{ll} are included in Table S1 and in Fig. 2. In all three cases, the bilayer tension $\Sigma = \Sigma_{ul} + \Sigma_{ll}$ is close to zero.

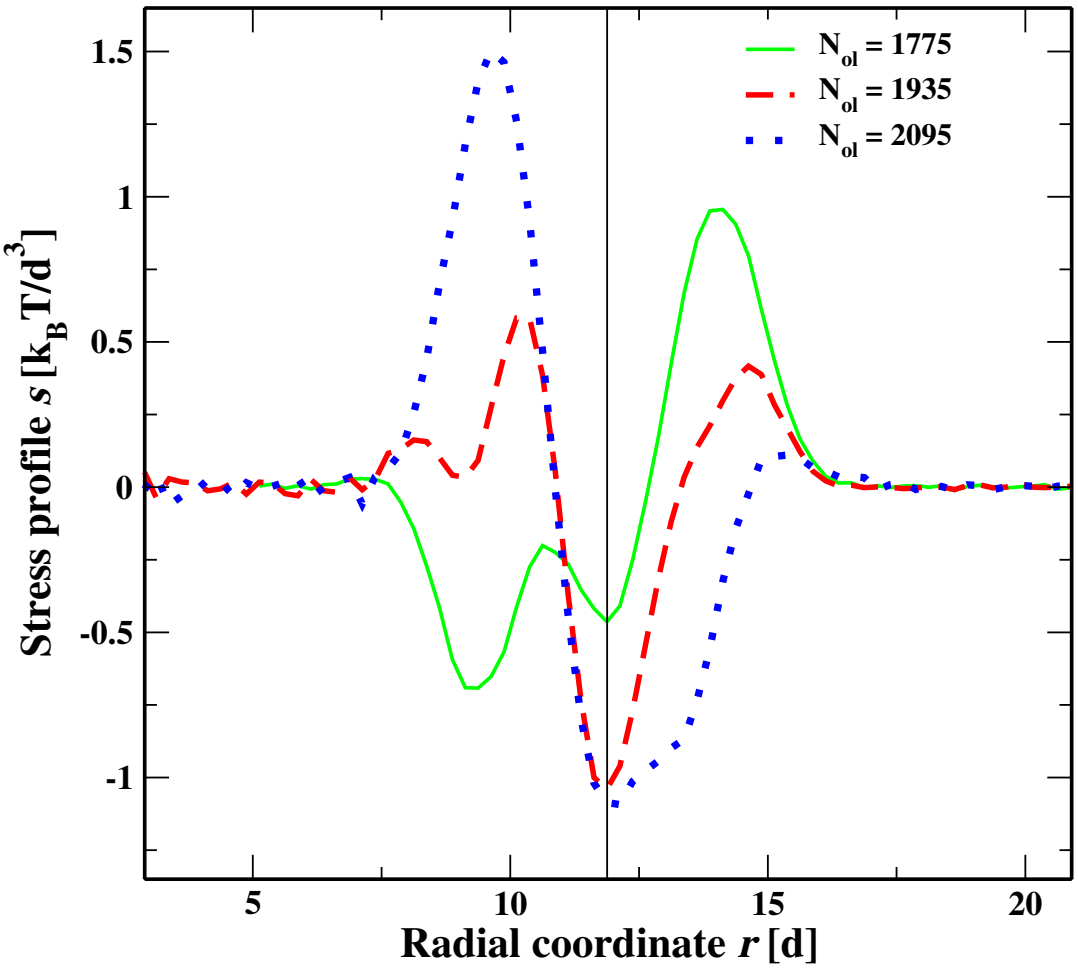

Figure S2: Stress profiles s across three spherical and tensionless bilayers that form nanovesicles with a diameter of $23.8\,d$ or 19 nm. The stress profiles are displayed as functions of the radial coordinate r, which measures the distance from the centers of the spheres. Each bilayer is assembled from N_{ol} lipids in the outer leaflet with $r > R_{\rm mid} = 11.88\,d$ and $N_{il} = 2875 - N_{ol}$ lipids in the inner leaflet with $r < R_{\rm mid}$. The three profiles are obtained for $N_{ol} = 1775$ (solid green line), corresponding to a stretched outer leaflet and a compressed inner one; $N_{ol} = 1935$ (dashed red line), corresponding to two leaflets with almost zero leaflet tensions; and $N_{ol} = 2095$ (dotted blue line) corresponding to a compressed outer leaflet and a stretched inner one. The numerical values of the corresponding leaflet tensions Σ_{ol} and Σ_{il} are included in Table S3 and Fig. 5. In all three cases, the bilayer tension $\Sigma = \Sigma_{ol} + \Sigma_{il}$ is close to zero.

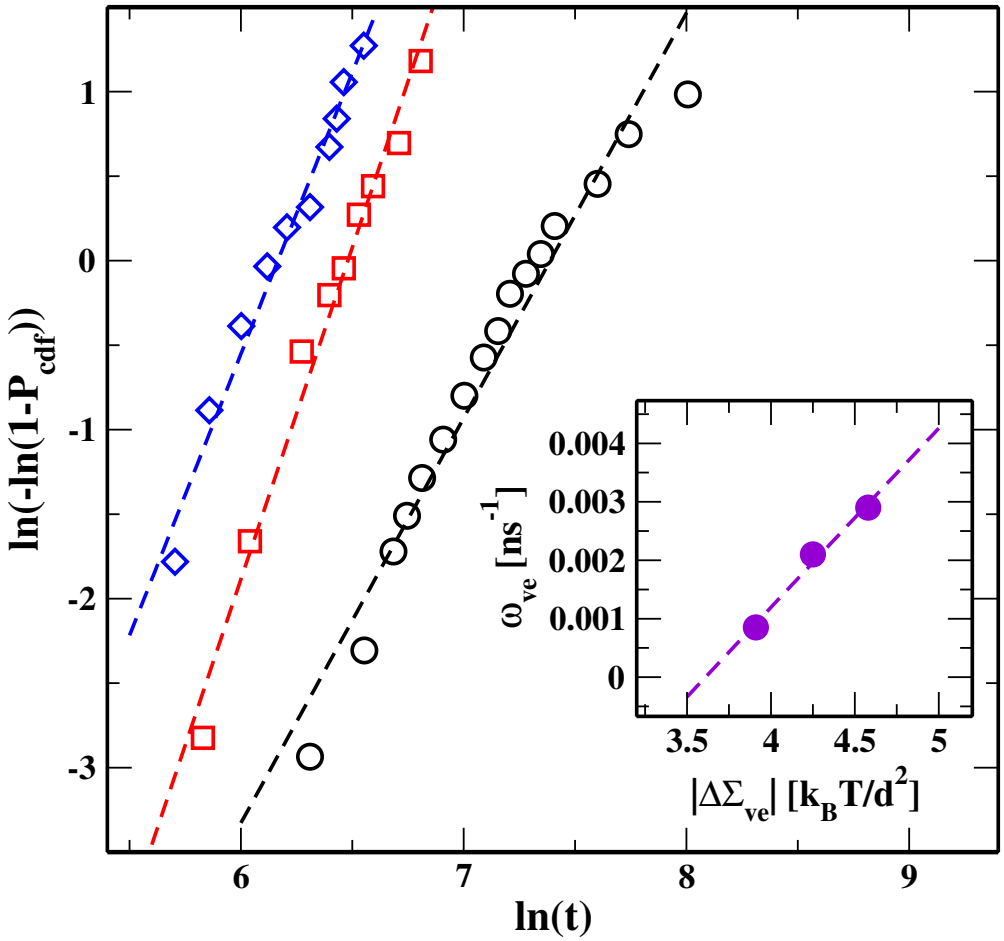

Figure S3: Weibull plots for the onset of flip-flops in the bilayer membranes of larger nanovesicles with a diameter of $23.8\,d$ or 19 nm. Three sets of data are displayed corresponding to $N_{ol} = 2105$ (black circles), $N_{ol} = 2125$ (red squares), and $N_{ol} = 2150$ (blue diamonds) lipids in the outer leaflet. All three data sets belong to the left instability regime in Fig. 5. The broken lines represent least square fits to the linear relations in eqn (12). The numerical values for the shape parameter k and the rate parameter $\omega_{\rm ve}$ are in Table S4. Inset: Monotonic increase of the rate parameter $\omega_{\rm ve}$ with the absolute value $|\Delta\Sigma_{\rm ve}| = |\Sigma_{ol} - \Sigma_{il}|$ of the stress asymmetry between the compressed outer and the stretched inner leaflets. The rate parameter $\omega_{\rm ve}$ is inversely proportional to the average flip-flop time and to the average life time of the metastable bilayer states.

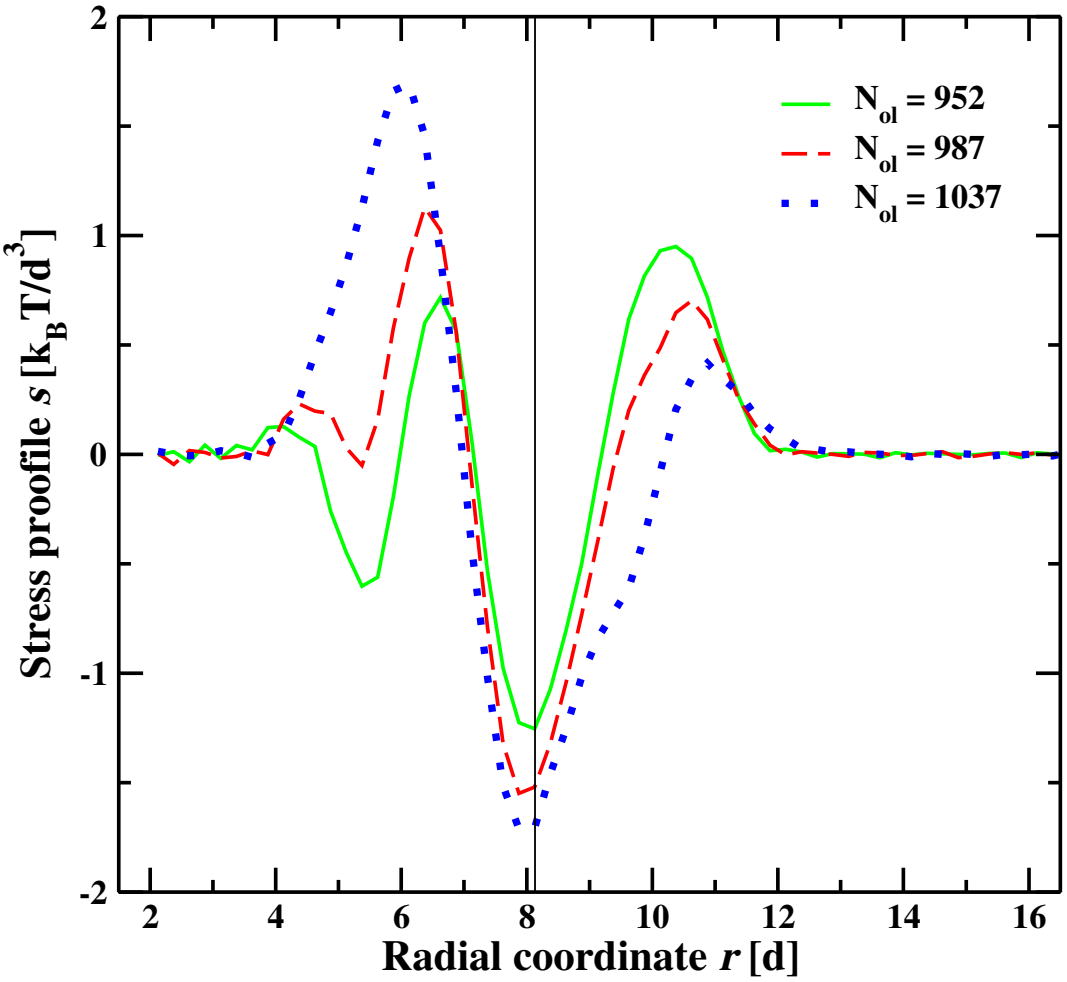

Figure S4: Stress profiles s across three spherical and tensionless bilayers that form smaller nanovesicles with a diameter of $16.3\,d$ or 13 nm. The stress profiles are displayed as functions of the radial coordinate r, which measures the distance from the centers of the spheres. Each bilayer is assembled from N_{ol} lipids in the outer leaflet with $r > R_{\rm mid} = 8.13\,d$ and $N_{il} = 1317 - N_{ol}$ lipids in the inner leaflet with $r < R_{\rm mid}$. The three profiles are obtained for $N_{ol} = 952$ (solid green line), corresponding to a stretched outer leaflet and a compressed inner one; $N_{ol} = 987$ (dashed red line), corresponding to two leaflets with almost zero leaflet tensions; and $N_{ol} = 1037$ (dotted blue line) corresponding to a compressed outer leaflet and a stretched inner one. The numerical values of the corresponding leaflet tensions Σ_{ol} and Σ_{il} are included in Table S5 and Fig. 6. In all three cases, the bilayer tension $\Sigma = \Sigma_{ol} + \Sigma_{il}$ is close to zero.

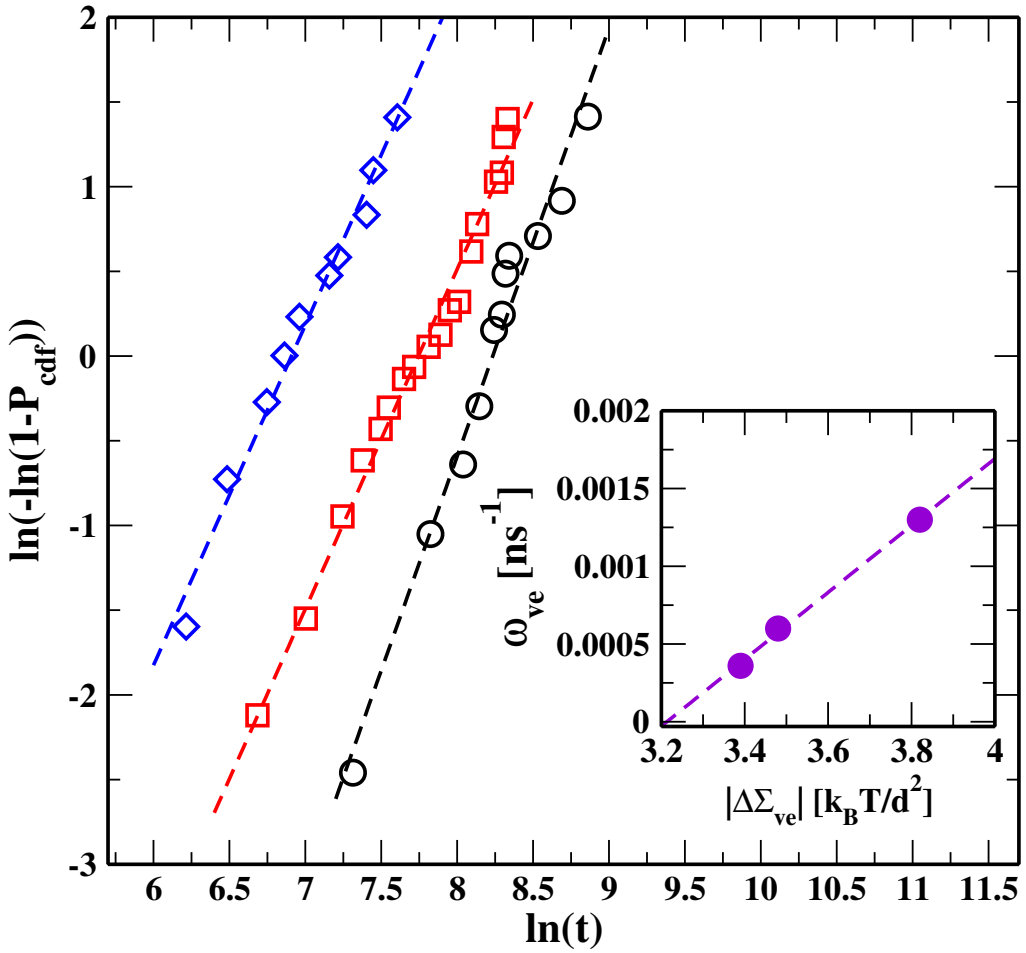

Figure S5: Weibull plots for the onset of flip-flops in the bilayer membranes of smaller nanovesicles with a diameter of 16.3 d or 13 nm. Three sets of data are displayed corresponding to $N_{ol} = 1041$ (black circles), $N_{ol} = 1046$ (red squares), and $N_{ol} = 1051$ (blue diamonds) lipids in the outer leaflets. All three data sets belong to the left instability regime in Fig. 8. The broken lines represent least square fits to the linear relations in eqn (12). The numerical values for the shape parameter k and the rate parameter $\omega_{\rm ve}$ are in Table S6. Inset: Monotonic increase of the rate parameter $\omega_{\rm ve}$ with the absolute value $|\Delta\Sigma_{\rm ve}| = |\Sigma_{ol} - \Sigma_{il}|$ of the stress asymmetry between the compressed outer and the stretched inner leaflets. The rate parameter $\omega_{\rm ve}$ is inversely proportional to the average flip-flop time which is equivalent to the average life time of the metastable bilayer states.

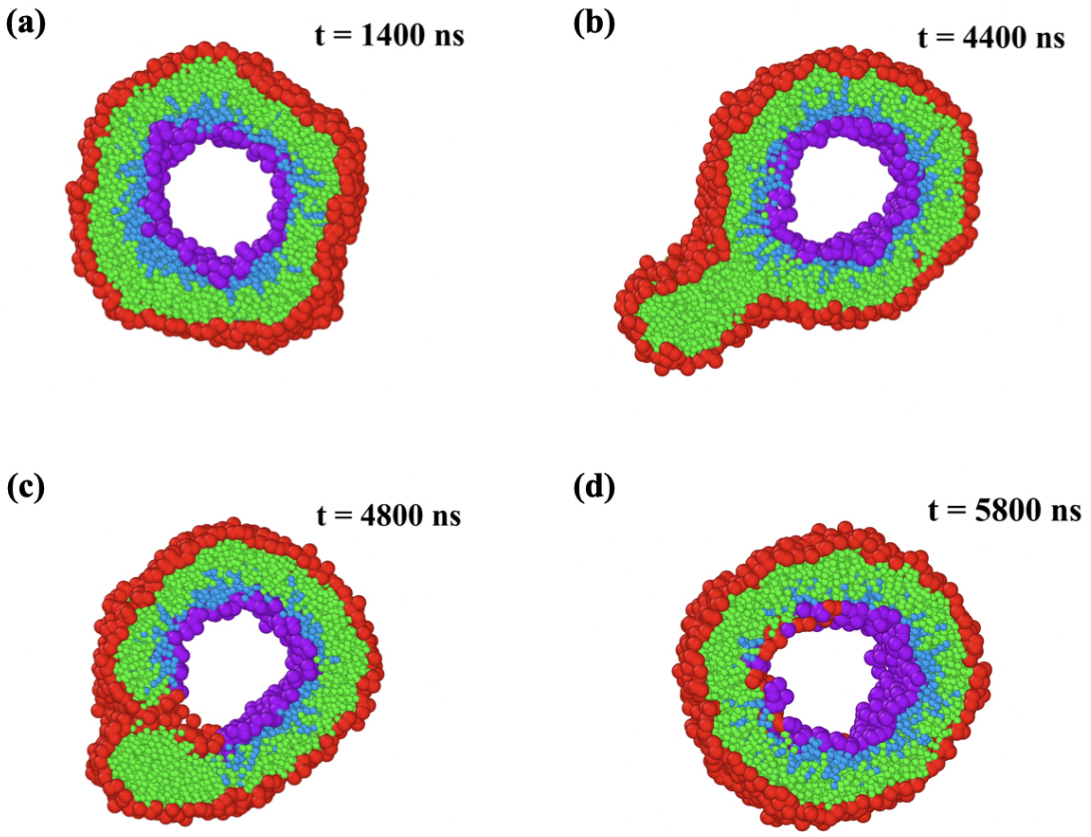

Figure S6: Structural instability and self-healing of a tensionless nanovesicle with a diameter of 13 nm. At time $t = 0$, the bilayer is assembled from $N_{ol} = 1041$ and $N_{il} = 276$ lipids which leads to a compressed outer leaflet with negative leaflet tension $\Sigma_{ol} = -1.68\, k_{\mathrm{B}}T/d^2$ and to pronounced shape fluctuations of the bilayer: (a) Snapshot of shape fluctuation at $t = 1400$ ns; (b) At $t = 4400$ ns, a cylindrical micelle has been formed from about 120 red-green lipids that were expelled from the outer leaflet; (c) At $t = 4800$ ns, lipids move towards the stretched inner leaflet along the contact line between micelle and bilayer; and (d) At $t = 5800$ ns, the self-healing process via this stress-induced lipid exchange has been completed and 57 red-green lipids have moved to the inner leaflet. The restored bilayer undergoes no further flip-flops until the end of our simulations at $t = 12.5\,\mu$s. For more details on the time course of this process, see time-lapse Movie 3. Color coding as in Fig. 1.

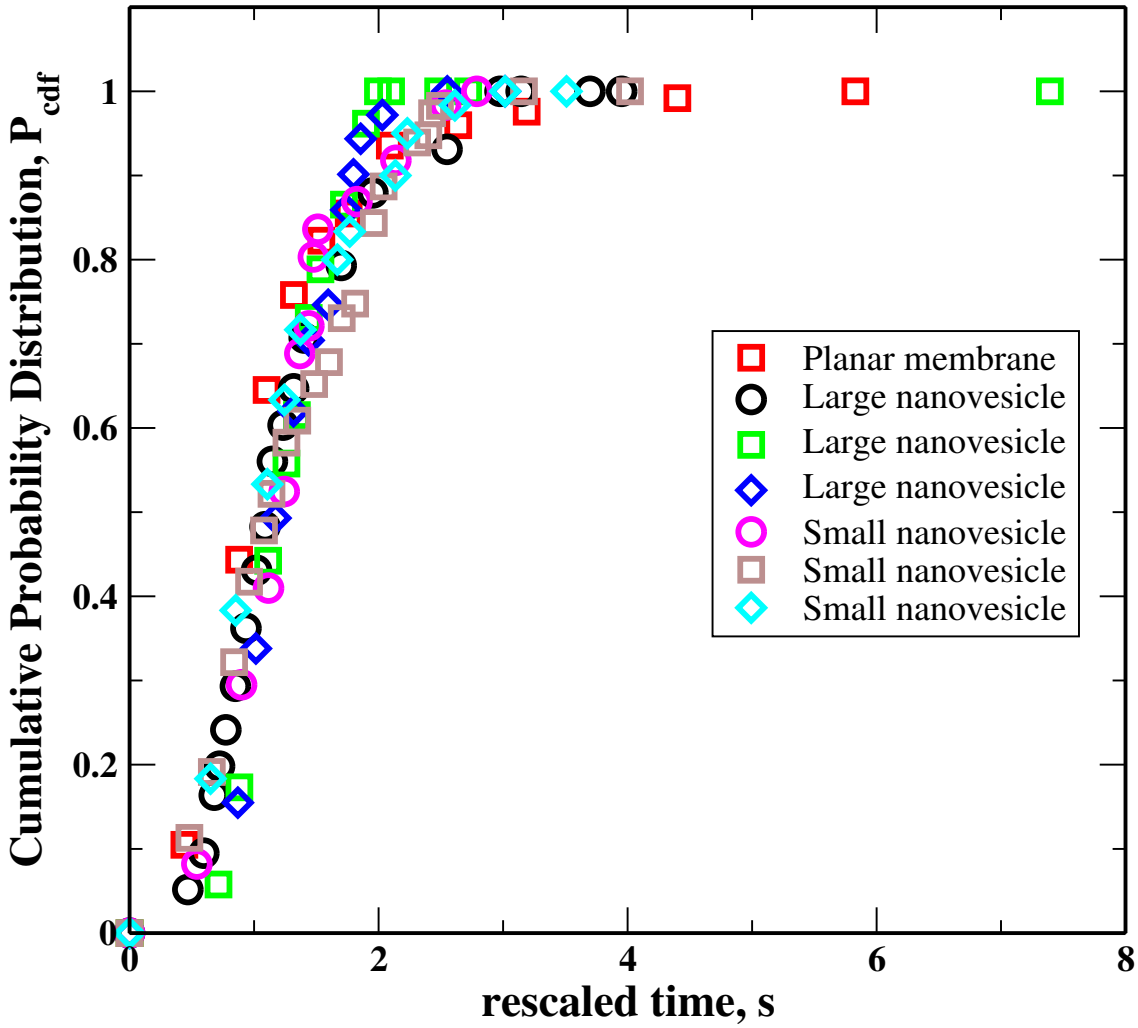

Figure S7: Cumulative distribution functions for the onset of flip-flops within the nanovesicles versus rescaled time $s = \omega_{\rm ve} t$. All six data sets for the large and small nanovesicles form a single master curve. For comparision, another data set (red squares) for the planar bilayer with $N_{ul} = 1015$ has also been included.

Supporting Tables for Planar Bilayers

Table S1: Metastable states and instability lines for planar bilayers; numerical parameter values for the data shown in Fig. 2: The bilayers are assembled from the lipid numbers N_{ul} and $N_{ll} = 1682 - N_{ul}$ in the upper and lower leaflet. For each lipid distribution, the data are obtained from three statistically independent simulations. The quantities a_{ul} and a_{ll} represent the areas per lipid in the upper and lower leaflet, respectively. The upper leaflet tension Σ_{ul} and the lower leaflet tension Σ_{ll} add up to the bilayer tension $\Sigma = \Sigma_{ul} + \Sigma_{ll}$, which is close to zero. Both leaflets are tensionless for the symmetric bilayer with $N_{ul} = N_{ll} = 841$ (6th row). Stress asymmetries between the two leaflets lead to nonzero values of the tension difference $\Delta\Sigma_{\rm pl} = \Sigma_{ul} - \Sigma_{ll}$ and of the torque density $\mathcal{T}_{\rm pl}$ as defined in eq 2. For $N_{ul} = 725$ (1st row) and $N_{ul} = 957$ (last row), corresponding to the two instability lines in Fig. 2, the bilayers start to undergo flip-flops. Areas are given in units of d^2 with the bead diameter d, tensions in units of $k_{\rm B}T/d^2$ with the thermal energy $k_{\rm B}T$.

N_{ul}	a_{ul} $[d^2]$	Σ_{ul} $[k_{\rm B}T/d^2]$	a_{ll} $[d^2]$	Σ_{ll} $[k_{\rm B}T/d^2]$	Σ $[k_{\rm B}T/d^2]$	$\Delta\Sigma_{\rm pl}$ $[k_{\rm B}T/d^2]$	$\mathcal{T}_{\rm pl}$ $[k_{\rm B}T/d]$
725	1.430	$+2.13 \pm 0.03$	1.083	-2.17 ± 0.06	-0.06	$+4.30$	$+9.34 \pm 0.11$
737	1.406	$+2.00 \pm 0.01$	1.097	-2.01 ± 0.02	$+0.01$	$+4.01$	$+7.62 \pm 0.10$
754	1.375	$+1.70 \pm 0.02$	1.117	-1.70 ± 0.02	0.00	$+3.40$	$+7.06 \pm 0.16$
783	1.312	$+1.15 \pm 0.01$	1.142	-1.20 ± 0.02	-0.04	$+2.35$	$+5.12 \pm 0.44$
812	1.261	$+0.55 \pm 0.01$	1.177	-0.60 ± 0.01	-0.04	$+1.15$	$+2.44 \pm 0.05$
841	1.217	-0.02 ± 0.01	1.217	0.00 ± 0.02	-0.01	-0.02	-0.06 ± 0.10
870	1.177	-0.64 ± 0.02	1.261	$+0.60 \pm 0.02$	-0.04	-1.24	-2.60 ± 0.28
899	1.142	-1.19 ± 0.02	1.312	$+1.16 \pm 0.00$	-0.04	-2.35	-4.75 ± 0.20
928	1.117	-1.74 ± 0.02	1.375	$+1.75 \pm 0.04$	$+0.02$	-3.49	-6.74 ± 0.57
945	1.097	-1.86 ± 0.30	1.406	$+1.86 \pm 0.20$	0.00	-3.72	-7.21 ± 1.01
957	1.083	-2.21 ± 0.05	1.43	$+2.17 \pm 0.02$	-0.04	-4.38	-9.01 ± 0.32

Table S2: Flip-flops in planar bilayers; numerical parameter values for the data in Fig. 3: Upper leaflet number N_{ul}, which determines the lower leaflet number $N_{ll} = 1682 - N_{ul}$; lipid area a_{ul} of the compressed upper leaflet, which implies the lipid area $a_{ll} = a_{ul}N_{ul}/N_{ll}$ of the stretched lower leaflet; leaflet tensions Σ_{ul} and Σ_{ll}; bilayer tension $\Sigma = \Sigma_{ul} + \Sigma_{ll}$; stress asymmetry $\Delta\Sigma_{\rm pl} = \Sigma_{ul} - \Sigma_{ll}$; and flip-flop rate $\omega_{\rm pl}$ in the instability regime, corresponding to the left shaded region in Fig. 2. The 2nd column provides the number of vesicles (#Ves) for which statistically independent simulations have been performed. Tensions and stress asymmetries are calculated in the metastable states before the first flip-flop. Units are given in terms of the bead diameter d and the thermal energy $k_{\rm B}T$.

N_{ul}	#Ves	a_{ul} d^2	Σ_{ul} $k_{\rm B}T/d^2$	Σ_{ll} $k_{\rm B}T/d^2$	Σ $k_{\rm B}T/d^2$	$\Delta\Sigma_{\rm pl}$ $k_{\rm B}T/d^2$	$\omega_{\rm pl}$ ns^{-1}
986	202	1.04	-2.33 ± 0.06	$+2.35 \pm 0.04$	$+0.02 \pm 0.03$	-4.68	0.002
1015	125	1.01	-3.02 ± 0.03	$+2.95 \pm 0.04$	-0.05 ± 0.04	-5.97	0.011
1073	126	0.95	-4.27 ± 0.08	$+4.31 \pm 0.12$	$+0.03 \pm 0.12$	-8.58	0.035

Supporting Tables for Larger Nanovesicles

Table S3: Metastable states and instability lines for larger nanovesicles with a diameter of $23.8\,d$ or 19 nm; numerical parameter values for the data in Fig. 5. The bilayers consist of an outer and an inner leaflet, which are assembled from N_{ol} and $N_{il} = 2875 - N_{ol}$ lipids. For each lipid distribution, the data are obtained from three statistically independent simulations. The outer and inner leaflets experience the leaflet tensions Σ_{ol} and Σ_{il}, respectively. The bilayer tension $\Sigma = \Sigma_{ol} + \Sigma_{il}$ is close to zero. Both leaflets are tensionless when the lipid number N_{ol} in the outer leaflet is larger than 1893 (6th row) and smaller than 1935 (7th row). Stress asymmetries between the two leaflets lead to nonzero values of the tension difference $\Delta\Sigma_{\rm ve} = \Sigma_{ol} - \Sigma_{il}$ and of the torque density $\mathcal{T}_{\rm ve}$ as defined in eqn (5). For $N_{ol} = 1755$ (first row) and $N_{ol} = 2105$ (last row), corresponding to the two instability lines in Fig. 5, the bilayers become unstable and start to undergo lipid flip-flops.

N_{ol}	a_{ol} $[d^2]$	Σ_{ol} $[k_{\rm B}T/d^2]$	a_{il} $[d^2]$	Σ_{il} $[k_{\rm B}T/d^2]$	Σ $[k_{\rm B}T/d^2]$	$\Delta\Sigma_{\rm ve}$ $[k_{\rm B}T/d^2]$	$\mathcal{T}_{\rm ve}$ $[k_{\rm B}T/d]$
1755	1.209	$+1.78 \pm 0.01$	1.236	-1.76 ± 0.05	$+0.02$	$+3.54$	$+8.66 \pm 0.38$
1775	1.195	$+1.60 \pm 0.01$	1.258	-1.54 ± 0.03	$+0.06$	$+3.14$	$+8.02 \pm 0.19$
1815	1.169	$+1.18 \pm 0.01$	1.306	-1.19 ± 0.02	-0.01	$+2.37$	$+5.63 \pm 0.06$
1861	1.140	$+0.68 \pm 0.01$	1.365	-0.70 ± 0.05	-0.02	$+1.38$	$+3.56 \pm 0.07$
1883	1.127	$+0.43 \pm 0.01$	1.395	-0.45 ± 0.02	-0.01	$+0.88$	$+2.31 \pm 0.23$
1893	1.121	$+0.33 \pm 0.01$	1.410	-0.37 ± 0.01	-0.04	$+0.70$	$+1.63 \pm 0.11$
1935	1.096	-0.17 ± 0.02	1.473	$+0.15 \pm 0.01$	-0.02	-0.32	-0.38 ± 0.29
1975	1.074	-0.63 ± 0.02	1.538	$+0.66 \pm 0.01$	$+0.03$	-1.29	-1.81 ± 0.32
2025	1.048	-1.20 ± 0.02	1.629	$+1.16 \pm 0.03$	-0.04	-2.36	-5.12 ± 0.07
2095	1.013	-1.94 ± 0.06	1.775	$+1.97 \pm 0.04$	$+0.04$	-3.91	-7.13 ± 0.67
2105	1.008	-1.97 ± 0.05	1.798	$+1.94 \pm 0.03$	-0.03	-3.91	-8.27 ± 0.31

Table S4: Flip-flops in larger nanovesicles; numerical parameter values for the data in Fig. 6: Lipid number N_{ol} in the outer leaflet, which determines the inner leaflet number $N_{il} = 2875 - N_{ol}$; area per lipid, a_{ol}, of the compressed outer leaflet; leaflet tensions Σ_{ol} and Σ_{il} in the outer and inner leaflets; bilayer tension $\Sigma = \Sigma_{ol} + \Sigma_{il}$; stress asymmetry $\Delta\Sigma_{\rm ve} = \Sigma_{ol} - \Sigma_{il}$; rate parameter $\omega_{\rm ve}$ and shape parameter k as obtained from fits of the data in Fig. S3 to the Weibull distribution in eqn (4). The 2nd column provides the number of vesicles (#Ves) for which statistically independent simulations have been performed. Tensions and stress asymmetries are calculated in the metastable bilayer states before the first flip-flop. Areas and tensions are given in units of bead diameter d and thermal energy $k_{\rm B}T$.

N_{ol}	#Ves	a_{ol} d^2	Σ_{ol} $k_{\rm B}T/d^2$	Σ_{il} $k_{\rm B}T/d^2$	Σ $k_{\rm B}T/d^2$	$\Delta\Sigma_{\rm ve}$ $k_{\rm B}T/d^2$	$\omega_{\rm ve}$ ns^{-1}	k
2105	126	1.203	-1.97 ± 0.05	$+1.94 \pm 0.03$	-0.03 ± 0.01	-3.91	0.0009	2.39
2125	70	1.191	-2.14 ± 0.04	$+2.11 \pm 0.06$	-0.036 ± 0.03	-4.25	0.0021	3.92
2150	72	1.177	-2.30 ± 0.12	$+2.28 \pm 0.10$	-0.026 ± 0.06	-4.58	0.0029	3.33

Supporting Tables for Smaller Nanovesicles

Table S5: Metastable states and instability lines for smaller nanovesicles with a diameter of $16.3\,d$ or 13 nm; numerical parameter values for the data in Fig. 8: The bilayers consist of an outer and an inner leaflet, which are assembled from N_{ol} and $N_{il} = 1317 - N_{ol}$ lipids. For each lipid distribution, the data are obtained from three statistically independent simulations. The outer and inner leaflets experience the leaflet tensions Σ_{ol} and Σ_{il}, respectively. The bilayer tension $\Sigma = \Sigma_{ol} + \Sigma_{il}$ is close to zero. Both leaflets are tensionless when the lipid number N_{ol} in the outer leaflet is larger than 977 (5th row) and smaller than 987 (6th row). Stress asymmetries between the two leaflets lead to nonzero values of the tension difference $\Delta\Sigma_{\rm ve} = \Sigma_{ol} - \Sigma_{il}$ and of the torque density $\mathcal{T}_{\rm ve}$ as defined in eqn (5). For $N_{ol} = 947$ (first row) and $N_{ol} = 1041$ (last row), corresponding to the two instability lines in Fig. 6, the bilayers become unstable and start to undergo lipid flip-flops.

N_{ol}	a_{ol} $[d^2]$	Σ_{ol} $[k_{\rm B}T/d^2]$	a_{il} $[d^2]$	Σ_{il} $[k_{\rm B}T/d^2]$	Σ $[k_{\rm B}T/d^2]$	$\Delta\Sigma_{\rm ve}$ $[k_{\rm B}T/d^2]$	$\mathcal{T}_{\rm ve}$ $[k_{\rm B}T/d]$
947	1.134	$+0.79 \pm 0.01$	1.546	-0.83 ± 0.02	-0.04	$+1.62$	$+3.54 \pm 0.19$
952	1.128	$+0.72 \pm 0.01$	1.567	-0.66 ± 0.03	$+0.06$	$+1.38$	$+4.19 \pm 0.26$
957	1.122	$+0.61 \pm 0.02$	1.589	-0.59 ± 0.03	$+0.02$	$+1.20$	$+3.27 \pm 0.47$
967	1.111	$+0.37 \pm 0.03$	1.635	-0.33 ± 0.01	$+0.04$	$+0.70$	$+2.20 \pm 0.40$
977	1.099	$+0.12 \pm 0.02$	1.683	-0.03 ± 0.03	$+0.08$	$+0.15$	$+1.30 \pm 0.14$
987	1.088	-0.11 ± 0.01	1.734	$+0.13 \pm 0.02$	$+0.02$	-0.24	-0.14 ± 0.15
997	1.077	-0.37 ± 0.01	1.788	$+0.46 \pm 0.02$	$+0.09$	-0.83	-0.80 ± 0.18
1007	1.067	-0.63 ± 0.01	1.846	$+0.64 \pm 0.01$	$+0.02$	-1.27	-2.48 ± 0.21
1017	1.056	-0.86 ± 0.01	1.907	$+0.94 \pm 0.01$	$+0.07$	-1.80	-3.02 ± 0.17
1027	1.046	-1.10 ± 0.01	1.97	$+1.14 \pm 0.02$	$+0.04$	-2.24	-4.42 ± 0.25
1037	1.036	-1.33 ± 0.04	2.04	$+1.33 \pm 0.01$	$+0.03$	-2.66	-5.34 ± 0.08
1041	1.032	-1.68 ± 0.01	2.07	$+1.71 \pm 0.02$	$+0.03$	-3.39	-5.40 ± 0.01

Table S6: Flip-flops in smaller nanovesicles; numerical parameter values for the data in Fig. 9: Lipid number N_{ol} in the outer leaflet, which determines the inner leaflet number $N_{il} = 1317 - N_{ol}$; area per lipid, a_{ol}, of the compressed outer leaflet; leaflet tensions Σ_{ol} and Σ_{il} in the outer and inner leaflets; bilayer tension $\Sigma = \Sigma_{ol} + \Sigma_{il}$; stress asymmetry $\Delta\Sigma_{\rm ve} = \Sigma_{ol} - \Sigma_{il}$; rate parameter $\omega_{\rm ve}$ and shape parameter k as obtained from fits to the Weibull distribution in eqn (4). The 2nd column provides the number of vesicles (#Ves) for which statistically independent simulations have been performed. Tensions and stress asymmetries are calculated for the metastable bilayer states before the first flip-flop. Units are given in terms of the bead diameter d and the thermal energy $k_{\rm B}T$.

N_{ol}	#Ves	a_{ol} d^2	Σ_{ol} $k_{\rm B}T/d^2$	Σ_{il} $k_{\rm B}T/d^2$	Σ $k_{\rm B}T/d^2$	$\Delta\Sigma_{\rm ve}$ $k_{\rm B}T/d^2$	$\omega_{\rm ve}$ ns^{-1}	k
1041	62	1.280	-1.68 ± 0.01	$+1.71 \pm 0.02$	0.03 ± 0.02	-3.39	0.0004	2.5
1046	116	1.273	-1.70 ± 0.01	$+1.78 \pm 0.01$	0.08 ± 0.01	-3.48	0.0006	2.0
1051	61	1.267	-1.88 ± 0.02	$+1.94 \pm 0.03$	0.05 ± 0.04	-3.82	0.0013	2.0

Supporting Table for Comparison of Different Systems

Table S7: Stability regimes together with the left and right instability lines, as displayed in Fig.s 2, 5, and 8, in terms of the torque density $\mathcal{T}_{\rm pl}$ for the planar bilayers and of the torque density $\mathcal{T}_{\rm ve}$ for the nanovesicles. The torque densities are given in units of $\delta \equiv k_{\rm B}T/d$.

	Left instability line	Stability regime	Right instability line
Planar bilayers	$\mathcal{T}_{\rm pl} = -9.01\,\delta$	$-7.21\,\delta \leq \mathcal{T}_{\rm pl} \leq +7.62\,\delta$	$\mathcal{T}_{\rm pl} = +9.34\,\delta$
Large nanovesicles	$\mathcal{T}_{\rm ve} = -8.27\,\delta$	$-7.13\,\delta \leq \mathcal{T}_{\rm ve} \leq +8.02\,\delta$	$\mathcal{T}_{\rm ve} = +8.66\,\delta$
Small nanovesicles	$\mathcal{T}_{\rm ve} = -5.40\,\delta$	$-5.34\,\delta \leq \mathcal{T}_{\rm ve} \leq +4.19\,\delta$	$\mathcal{T}_{\rm ve} = +3.54\,\delta$

Movie captions

Movie 1: Structural instability and self-healing of a tensionless planar bilayer, initially assembled from $N_{ul} = 986$ red-green lipids in the compressed upper leaflet and $N_{ll} = 696$ purple-blue lipids in the stretched lower leaflet. The bilayer first bulges towards the upper leaflet, which then undergoes a structural instability by expelling about 100 red-green lipids that form a globular micelle in contact with the upper leaflet. After about 1000 ns, the red-green lipids start to undergo flip-flops along the contact line between micelle and bilayer towards the stretched lower leaflet. These flip-flops lead to a self-healing process that is completed after 1700 ns. The restored bilayer contains 93 red-green lipids in its lower leaflet and remains in a long-lived metastable state without flip-flops until the end of the simulations.

Movie 2: Sructural instability and self-healing of a large nanovesicle with a diameter of 19 nm. The tensionless bilayer of the nanovesicle is initially assembled from $N_{ol} = 2105$ red-green lipids in the compressed outer leaflet and $N_{il} = 770$ purple-blue lipids in the stretched inner leaflet. The bilayer first undergoes pronounced shape fluctuations which have a 'kinky' appearance and then forms a cylindrical micelle from about 180 red-green lipids that are expelled from the outer leaflet. After about 1700 ns, the red-green lipids start to undergo flip-flops towards the stretched inner along the contact line between micelle and bilayer. These flip-flops drive a self-healing process that is completed after 2710 ns. The restored bilayer contains 111 red-green lipids in its inner leaflet and remains in a long-lived metastable state without flip-flops until the end of the simulations.

Movie 3: Structural instability and self-healing process of a small nanovesicle with a diameter of 13 nm. The tensionless bilayer of the nanovesicle is initially assembled from $N_{ol} = 1041$ red-green lipids in the compressed outer leaflet and $N_{il} = 276$ purple-blue lipids in the stretched inner leaflet. The bilayer first undergoes pronounced shape fluctuations which have a 'kinky' appearance and then forms a cylindrical micelle from about 120 red-green lipids that are expelled from the outer leaflet. After about 4700 ns, the red-green lipids start to undergo flip-flops towards the stretched inner leaflet along the contact line between micelle and bilayer. These flip-flops drive a self-healing process that is completed after 5800 ns. The restored bilayer contains 57 red-green lipids in its inner leaflet and remains in a long-lived metastable state without flip-flops until the end of the simulations.